Effects of Pressure on the Magnetic Properties of MnAs

N. MENYUK, J. A. KAFALAS, K. DWIGHT, AND J. B. GOODENOUGH
Lincoln Laboratory, Massachusetts Institute of Technology, Lexington, Massachusetts 02173*
(Received 16 August 1968)

Using a vibrating-coil magnetometer, we have studied the effect of hydrostatic pressures of up to 11 kbar on the magnetic properties of MnAs. These experiments were carried out between 60 and 500°K. The boundary between the ferromagnetic hexagonal ($B8_1$) phase and the orthorhombic ($B31$) phase has been determined. In addition, the existence of ordered metamagnetic and ferromagnetic structures within the high-pressure $B31$ phase is established and their boundaries delineated in the pressure-temperature phase space. The existence of regions within this space in which the paramagnetic susceptibility of the $B8_1$ and $B31$ phases follow a Curie-Weiss law has enabled us to confirm directly the hypothesis of Goodenough, Ridgley, and Newman that the manganese moment goes from a low-spin to a high-spin configuration on going from the $B31$ to the $B8_1$ phase. The pressure dependence of the paramagnetic Curie point ($d\theta/dp$) was found to be negative in the $B8_1$ phase and positive in the $B31$ phase. This is shown to be in contradiction with the Bean-Rodbell model as it has been applied to MnAs. We show that the minimum generalization of their model to permit consistency with our results requires consideration of multiple exchange interactions, anisotropic strain effects, and higher-order contributions to the elastic energy. Finally, we give an interpretation of our results within the framework of the band spectrum of MnAs.

I. INTRODUCTION

WE have investigated the effects of hydrostatic pressure on the magnetic properties of MnAs. The measurements, as described in this paper, have been carried out at pressures up to 11 kbar and cover a temperature interval from approximately 60 to almost 500°K.

At atmospheric pressure, manganese arsenide is ferromagnetic at low temperature and exhibits a discontinuous loss of ferromagnetism at about 40°C (T_1). Above this temperature the inverse susceptibility decreases with increasing temperature to 126°C (T_2), after which the inverse susceptibility curve obeys the Curie-Weiss relationship. The magnetization data, taken from measurements by Guillaud,[1] are summarized in Fig. 1.

The susceptibility behavior in the temperature region $40°C<T<126°C$ was ascribed to antiferromagnetism by Guillaud,[1] but a subsequent neutron diffraction study by Bacon and Street[2] showed no evidence of long-range order. However, the transition at 40°C was found to be accompanied by a discontinuous change in lattice dimensions[3,4] and by a transformation from the hexagonal NiAs structure ($B8_1$) below T_1 to the orthorhombic MnP structure ($B31$) above T_1[4]. The orthorhombic $B31$ phase in MnAs involves small displacements of the ions from their position in the hexagonal $B8_1$ phase. It was found[4] that on increasing the temperature above T_1, the orthohombic "distortion" decreased continuously until it disappeared at T_2, with a reversion to the $B8_1$ structure. However, unlike the first-order transformation at T_1, the transition at T_2 involves no discontinuities in the lattice parameter and is of higher order.

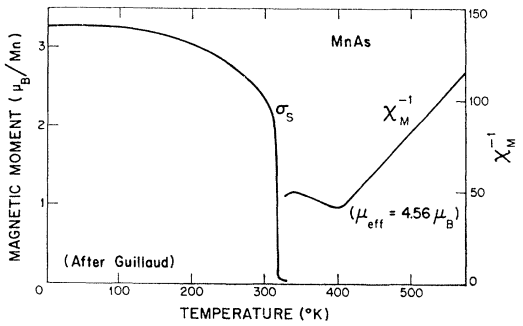

FIG. 1. Magnetic properties of MnAs at atmospheric pressure.

Bean and Rodbell[5,6] proposed that the effect at 40°C was a first-order ferromagnetic-paramagnetic phase transformation. They presented a thermodynamic theory in which the magnetic energy was treated within the molecular field approximation; it showed that such a transformation could occur in a compressible material with a strain-dependent exchange energy. This dependence was expressed by the equation

$$T_c = T_0[1+\beta(V-V_0)/V_0], \qquad (1)$$

where T_c is the Curie temperature, T_0 would be the Curie temperature if the lattice were incompressible, V is the volume, and V_0 is the volume in the absence of exchange interactions. They were able to obtain values for the strain sensitivity of magnetic exchange (β) and for the compressibility that were consistent with their magnetic data. In a later work, DeBlois and Rodbell[7] determined the transformation temperature as a function of pressure and magnetic field, using

* Operated with support from the U. S. Air Force.
[1] C. Guillaud, J. Phys. Radium **12**, 223 (1951).
[2] G. E. Bacon and R. Street, Nature **175**, 518 (1955).
[3] B. T. M. Willis and H. P. Rooksby, Proc. Phys. Soc. (London) **B67**, 290 (1954).
[4] R. H. Wilson and J. S. Kasper, Acta Cryst. **17**, 95 (1964).
[5] C. P. Bean and D. S. Rodbell, Phys. Rev. **126**, 104 (1962).
[6] D. S. Rodbell and C. P. Bean, J. Appl. Phys. Suppl. **33**, 1037 (1962).
[7] R. W. DeBlois and D. S. Rodbell, Phys. Rev. **130**, 1347 (1963).

pressures up to 1 kbar and applied fields up to 110 kOe, and obtained apparent agreement with the strain-dependency theory.

Bean and Rodbell[5] ascribed the susceptibility maximum above T_1 to the onset of the orthorhombic distortion. However, Goodenough, Ridgley, and Newman[8] pointed out that the two crystallographic phases of MnAs could reflect two distinct spin states of manganese, with the $B8_1$ phase corresponding to a high-spin manganese configuration and the $B31$ phase corresponding to the low-spin manganese configuration. Measurements performed on the compound $MnAs_{0.9}P_{0.1}$ tended to confirm this interpretation, but were subject to the criticism that the volume changes were achieved by chemical rather than physical means. In a later paper, Goodenough and Kafalas[9] determined the $B8_1 \leftrightarrow B31$ phase transitions as functions of both temperature and pressure by measuring the resistivity discontinuity that is known to accompany the transformation.[1] Their results indicated that the principal effect of phosphorous substitution was the accompanying change in molecular volume, which lent additional support to the conclusion that the transition is accompanied by a change in spin state. They pointed out that this did not negate the Bean-Rodbell theory, but required that the physical interpretation of the parameter β be expanded to include the volume dependence of magnetic moment as well as the interatomic exchange energy. They also emphasized that the change from one spin state to another occurs in a relatively narrow temperature interval and requires an abrupt change in the intra-atomic exchange splitting at some critical value of the lattice parameters.

In this paper we describe our study of the magnetic moment of MnAs as a function of pressure, temperature, and applied field. For this purpose we have used a vibrating-coil magnetometer in conjunction with a hydrostatic pressure-generating system, as described in Sec. II. The results of these measurements, which are given in Sec. III, have enabled us to establish and delineate the complicated magnetic phase structure of both the hexagonal and orthorhombic phases of MnAs. They have also served to directly confirm the existence of a change in the magnetic moment of the manganese ion at the $B8_1$-B31 transition. In Sec. IV, after showing that the Bean-Rodbell model in its present form cannot be applied to the first-order transition in MnAs, we generalize their model and determine minimum requirements for consistency with our results. Finally, in Sec. V, we consider the interpretation of our results in terms of the band spectrum of MnAs.

[8] J. B. Goodenough, D. H. Ridgley, and W. A. Newman, in *Proceedings of the International Conference on Magnetism, Nottingham, 1964* (The Institute of Physics and The Physical Society, London, 1965).

[9] J. B. Goodenough and J. A. Kafalas, Phys. Rev. **157**, 389 (1967).

II. EXPERIMENTAL TECHNIQUE

The magnetic measurements were made using a vibrating-coil magnetometer (VCM).[10,11] This magnetometer converts the dipole moment of a sample placed in a magnetic field into an electrical signal by vibrating a pickup coil along the dipole axis. Since there is no physical contact between the vibrating coil and the sample, there is complete freedom in altering the sample environment. However, the pickup-coil signal also measures the dipole-moment contribution of the Dewar (or furnace) and the pressure vessel. Therefore it is important that the magnetic moment of these items be temperature-independent and as small as possible. Their contribution must be considered in the final data reduction.

The effect of the Dewar has been minimized by making the Dewar tail of oxygen-free high-conductivity (OFHC) copper, while the pressure vessel is made of a diamagnetic copper-beryllium alloy.[12] The experimental arrangement is shown in Fig. 2.

A pressure-generating unit capable of generating 200 000 psi of pressure with helium gas was used. The pressure was measured with an accuracy of 0.5% and a reproducibility of 50 psi by using a manganin wire resistance in the high-pressure system as one leg of a Wheatstone Bridge. Experiments were carried out at pressures up to 11 kbar. However, above 400°K, the pressure was limited to 3 kbar since beryllium copper loses tensile strength at higher temperatures.[13] The experiments described in this paper were carried out between 60 and 500°K, in applied magnetic fields up to 10 kOe.

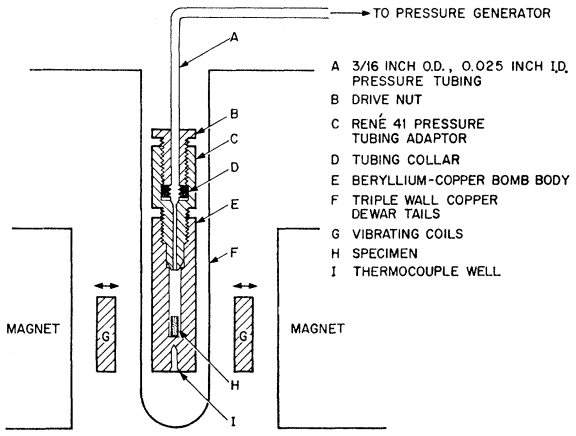

FIG. 2. Experimental arrangement for experiments conducted at and below room temperature.

[10] D. O. Smith, Rev. Sci. Instr. **27**, 261 (1956).

[11] K. Dwight, N. Menyuk, and D. Smith, J. Appl. Phys. **29**, 491 (1958).

[12] It should be noted that Cu-Be alloys contain a considerable amount of transition metal additives and are not, in general, diamagnetic. However, alloy 125, manufactured by the Brush Beryllium Co., is diamagnetic. We have checked this claim over the temperature interval covered in this experiment.

[13] K. G. Wikle and N. P. Sarle, Mater. Res. Std. **61**, 988 (1961).

III. EXPERIMENTAL RESULTS

A. $B8_1 \rightleftarrows B31$ Transition

The boundaries between the $B8_1$ and $B31$ structures of MnAs were determined by measuring the magnetic moment of the sample as a function of pressure at constant temperature. These measurements were carried out in an applied field of 100 Oe. A typical result of these measurements, obtained at 201°K, is shown in Fig. 3. It is seen that on increasing the pressure there is a value above which the magnetic moment drops sharply, thereby demarcating the $B8_1 \rightarrow B31$ phase transition (~4 kbar in this case). However, on then decreasing the pressure, a large hysteresis effect is observed, with the $B31 \rightarrow B8_1$ transition not occurring until the pressure is below 2 kbar.

The transition pressures are arbitrarily chosen as those at which the magnetic moment is half its atmospheric value, and the results of a large number of such measurements, carried out between 70 and 313°K, lead to the phase diagram shown in Fig. 4. These results are in essential accord with the corresponding curve obtained by Goodenough and Kafalas[9] from resistivity measurements. The only significant difference is the observation that the $B8_1 \rightarrow B31$ transition pressure is decreasing with decreasing temperature at a rate of $dT_1/dP = 83.5$°C/kbar below 180°K. To determine whether this corresponds to a constant-volume transition requires a knowledge of the compressibility K and the coefficient of thermal expansion α in MnAs. These quantities have not been measured directly, but analysis on the basis of the Bean-Rodbell theory by DeBlois and Rodbell[7] led them to assign the values 4.55×10^{-12} $(\text{dyn/cm}^2)^{-1}$ and $5.71\times10^{-5}(°\text{C})^{-1}$ for K and α, respectively. Assuming these to be the correct values leads to a predicted pressure dependence of transition temperature $dT_1/dP = 80.7$°C/kbar. In view of the inapplicability of the Bean-Rodbell theory in its present form to the MnAs transition, as discussed in Sec. IV, this excellent agreement between experiment and prediction must be treated as fortuitous. However, it serves to indicate that the rate of change of pressure with temperature is consistent with an isovolumetric transition below 180°K.

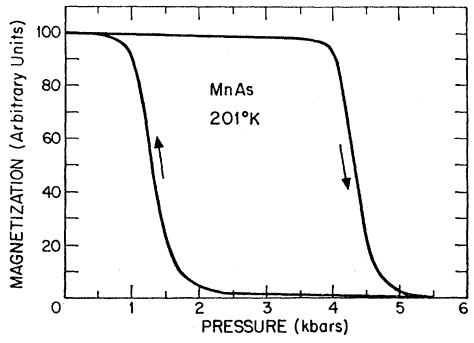

FIG. 3. Typical isothermal curve showing variation of magnetization with pressure through $B8_1 \leftrightarrow B31$ transitions in applied magnetic field of 100 Oe.

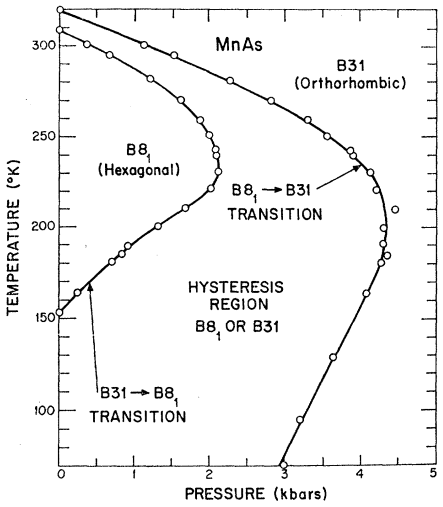

FIG. 4. Variation of $B8_1 \rightarrow B31$ and $B31 \rightarrow B8_1$ transition pressures as functions of temperature. Transition pressure taken as that pressure at which magnetization is one-half its atmospheric pressure value.

There are enough experimental points in Fig. 4 to definitively establish that the $B8_1$-$B31$ transition pressure is a smoothly varying function of temperature. This disagrees with the conclusion of Grazhdankina and Bersenev,[14] who studied the pressure dependence of this transition in the high-temperature region. They concluded there were two distinct types of phase transition involved,[15] one in the temperature range $270°\text{K} < T < 314°\text{K}$ with $dT_1/dP = -16.5$°C/kbar and a second between 250 and 270°K, with $dT_1/dP = -35$°C/kbar.

B. Magnetic Order in Orthorhombic MnAs

Measurements of the magnetic moment μ of the MnAs sample in the high-pressure ($B31$) phase were made as a function of temperature for several values of pressure and applied magnetic field. The results for eight different pressures obtained between room temperature and ~60°K in a field of 10 kOe are given in Fig. 5.

[14] N. P. Grazhdankina and Yu. S. Bersenev, Zh. Eksperim. i Teor. Fiz. **51**, 1052 (1966) [English transl.: Soviet Phys.—JETP **24**, 702 (1967)].

[15] Their conclusion of two distinct phase transitions can be understood with the help of Figs. 3 and 4. Grazhdankina and Bersenev performed their experiments by varying the temperature under nominally isobaric conditions and observing the difference in the induction emf on passing through the transition temperatures. At low pressures they observed the full change from $B8_1$ to $B31$ to $B8_1$ on varying the temperature. However, it can be seen from Fig. 4 that if MnAs is in the $B31$ phase at a pressure significantly greater than 2 kbar, the sample will not go into the $B8_1$ phase completely. However, as seen in Fig. 3, there is a finite pressure region over which there will be a partial transformation, which will be evidenced by a small change in the induction emf. It was the appearance of this reduction in the change of the induction emf with increasing pressure that led Grazhdankina and Bersenev to postulate the existence of a second type of phase transition.

The local maxima observed in the temperature region ~230—240°K indicate the onset of antiferromagnetic long-range order. Taking the temperature of the local maximum as the Néel point T_N, we have determined T_N as a function of pressure at 10 and 1 kOe, with the results shown in Fig. 6. The 1-kOe curve is limited at the low-pressure end because the local maximum of the μ-versus-T curve is extremely shallow in this field at 4 kbar, and below this pressure the onset of long-range order is evidenced only by a change in the slope of the curve. Conversely, the 10-kOe curve is limited at the high-pressure end of the curve by the appearance of a large moment below T_N, as is seen in Fig. 5. This effect skews the local maximum at high pressures. Above 9 kbar at 10 kOe, the rising moment overtakes T_N.

The curve of T_N versus pressure, as given in Fig. 6, indicates two approximately linear regions, with $dT_N/dP=4.0$ and 1.4°K/kbar for pressures less than or greater than 5 kbar, respectively. Grazhdankina and Bersenev[14] also noted the presence of a Néel point in the high-pressure phase of MnAs, reporting a pressure dependence $dT_N/dP=2.2$°K/kbar on the basis of measurements made between approximately 4 and 9 kbar.

In a "normal" polycrystalline antiferromagnet below T_N, the magnetic moment decreases with decreasing temperature. Therefore, the observed increase in μ with decreasing temperature below T_N is indicative of either ferromagnetism or metamagnetism, and the sharp drop in μ with further reduction in temperature is characteristic of a ferromagnetic-antiferromagnetic transition. Similar behavior has been observed in the isostructural series $MnAs_{1-x}P_x$ for $x=0.1$,[8] and in a recent study by Roger and Fruchart[16] for $0.03<x<0.15$. This similarity appears to justify the assumption of Goodenough *et al.*,[8] that the principal effect of phosphorus substitution on the magnetic properties of MnAs will be equivalent to that of a lattice reduction.

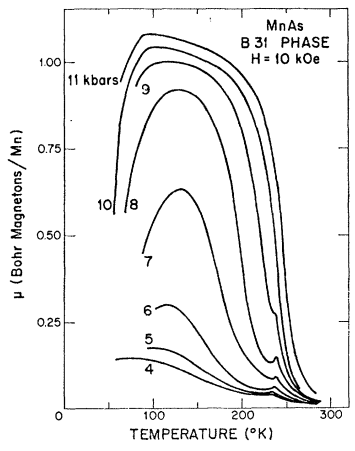

FIG. 5. Variation with temperature of the magnetic moment of MnAs in the orthorhombic phase at the indicated pressures in a magnetic field of 10 kOe.

[16] A. Roger and R. Fruchart, Mater. Res. Bull. **3**, 253 (1968).

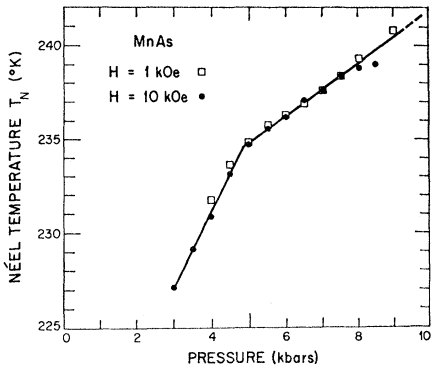

FIG. 6. Néel temperature of orthorhombic MnAs as a function of pressure in applied magnetic fields of 1 and 10 kOe.

As is seen in Fig. 5, the increase in μ with decreasing temperature rises sharply with increasing pressure. However, there is an apparent trend to saturation of this effect at the highest pressures achieved. In addition, a flattening of the magnetization curves, consistent with ferromagnetism, is observed at the higher pressures before the onset of the low-temperature transition. This aspect is further emphasized in Fig. 7, where the values of μ versus T at various applied fields are given for $P=9$ kbar. The apparent ferromagnetism in the intermediate-temperature region is illustrated in Fig. 8, as well as the metamagnetic behavior of MnAs at both higher [*Meta* (1)] and lower [*Meta* (2)] temperatures. These two regions are distinguished from each other by the fact that in state *Meta* (1) $dH_{cr}/dT>0$, while in state *Meta* (2) $dH_{cr}/dT<0$, where H_{cr} is the critical transition field for departure from antiferromagnetic behavior.

The magnetic behavior of orthorhombic MnAs immediately below T_N is similar to that observed in several rare-earth metals, such as dysprosium[17] and holmium,[18] where the magnetic structures are helical with temperature-dependent wavelength.[19,20] However, the analogy is a limited one, since increasing pressure decreases T_N in the rare-earth metals and also tends to depress the increase in moment observed below T_N in dysprosium,[21] which is opposite to the effect observed in MnAs. The abrupt low-temperature transition from ferromagnetism to metamagnetic state (2) has a counterpart in the ferromagnetic-metamagnetic transition of isostructural MnP at 50°K.[22]

Curves similar to those shown for $P=9$ kbar in Figs. 7 and 8 were obtained at other pressures. These

[17] J. F. Elliot, S. Legvold, and F. H. Spedding, Phys. Rev. **94**, 1143 (1954).
[18] B. L. Rhodes, S. Legvold, and F. H. Spedding, Phys. Rev. **109**, 1547 (1958).
[19] J. W. Cable, E. O. Wollan, W. C. Koehler, and M. K. Wilkinson, J. Appl. Phys. **32S** (1961).
[20] W. C. Koehler, J. W. Cable, E. O. Wollan, and M. K. Wilkinson, J. Phys. Soc. Japan Suppl. **17**, 32 (1962).
[21] L. B. Robinson, S. I. Tan, and K. F. Sterrett, Phys. Rev. **141**, 548 (1966).
[22] E. E. Huber, Jr., and D. H. Ridgley, Phys. Rev. **135**, A1033 (1964).

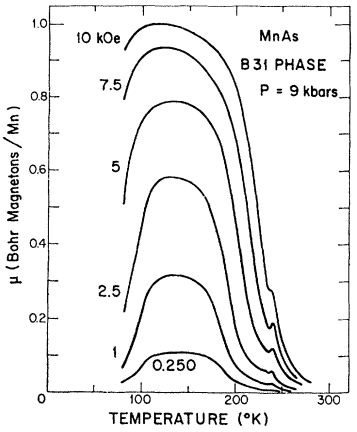

FIG. 7. Magnetic moment of orthorhombic MnAs at a pressure of 9 kbar as a function of temperature at the indicated magnetic field.

enabled us to define the region in P-T space in which orthorhombic MnAs is ferromagnetic. The boundary established for this region is shown in Fig. 9.

C. Paramagnetic Susceptibility Measurements

Paramagnetic measurements under varying pressure conditions have been made above T_2, where MnAs is in the hexagonal phase, and above T_N at higher pressures, where MnAs is orthorhombic. In order to distinguish between measurements in the two phases, we will use the notation $\chi(B8)$ and $\theta(B8)$ to refer to the susceptibility and paramagnetic Curie temperature, respectively, in the hexagonal phase, and $\chi(B31)$ and $\theta(B31)$ for their corresponding values in the orthorhombic phase.

Measurements in the hexagonal phase were limited to the temperature interval between T_2 and 500°K. At atmospheric pressure, T_2 is approximately 400°K, permitting measurement over a 100-deg interval. However, on increasing pressure, T_2 was found to increase rapidly. Over the pressure interval from one atmosphere to 3 kbar, we obtained the linear relationship $dT_2/dP = 23$°K/kbar. At higher pressures this reduced the temperature interval over which measurements could be made in the hexagonal phase, and thereby reduced the accuracy of the extrapolation-determined $\theta(B8)$.

The results of the measurements of the inverse susceptibility versus temperature at pressures of 1 atm and at 0.75, 1.5, and 2.25 kbar are summarized in Fig. 10. As shown in this figure, all four curves are consistent with a constant slope corresponding to $\mu_{\text{eff}}(B8) = 4.45\mu_B$ and to a pressure dependence of the paramagnetic Curie temperature $d\theta(\text{B8})/dP = -12$°K/kbar. Our results at atmospheric pressure are in good agreement with those of Guillaud.[1]

Additional paramagnetic measurements were made in the orthorhombic phase at pressures ranging from 4 to 10 kbar. At these higher pressures the temperature was limited by the strength of the bomb to a region from slightly above the Néel point to 400°K. The results, given in Fig. 11, show that immediately above the Néel point the inverse susceptibility in this pressure range follows a Curie-Weiss relationship. The effective moments $\mu_{\text{eff}}(B31)$ and paramagnetic Curie temperatures $\theta(B31)$ are given in Table I. The variation of $\mu_{\text{eff}}(B31)$ with pressure between 4 and 10 kbar is small and falls within the experimental uncertainty. The effective paramagnetic moment values of approximately $2\mu_B$ are consistent with the saturation moment value of slightly over $1\mu_B$ obtained in the ferromagnetic $B31$ state at 11 kbar. In addition, the positive value of $d\theta(B31)/dP = +7$°K/kbar, indicating a relative increase with pressure in ferromagnetic interactions, is consistent with the appearance at higher pressures of a ferromagnetic phase below the ordering temperature, as shown in Fig. 9.

There is a marked contrast in the paramagnetic behavior of the two phases. First, although the values of

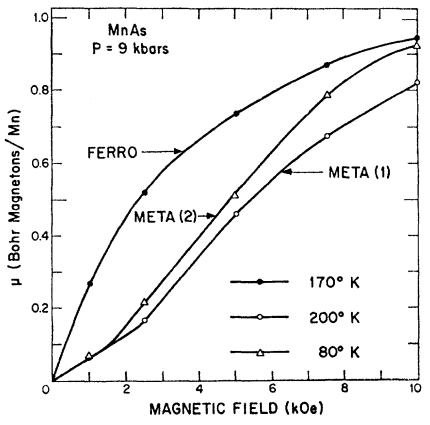

FIG. 8. Magnetic moment of orthorhombic MnAs at a pressure of 9 kbar as a function of applied magnetic field at the indicated temperatures. This figure illustrates how the high-pressure ferromagnetic state can be distinguished from the metamagnetic states at both higher and lower temperatures.

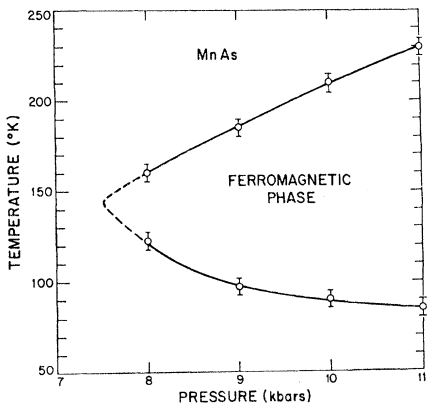

FIG. 9. Delineation of the region in the pressure-temperature phase space in which orthorhombic MnAs is ferromagnetic.

TABLE I. Paramagnetic properties of orthorhombic MnAs.

Pressure (kbar)	μ_{eff} (μ_B)	$\theta(B31)$ (°K)
5	1.91	220.5
6	1.87	228.0
7	1.83	238.0
8	2.02	242.5
9	2.02	248.5
10	2.06	256.0

μ_{eff} appear to be nearly constant within each phase, there is a change from $4.55\mu_B$ to approximately $2\mu_B$ on going from the hexagonal to the orthorhombic phase. This establishes that virtually the entire change in μ_{eff} occurs within the narrow temperature interval below T_2 where the susceptibility decreases with increasing temperature. This directly confirms the hypothesis of Goodenough, Ridgley, and Newman[8] that the crystallographic transformation from the high-temperature $B8_1$ structure to the $B31$ structure is accompanied by a change from a high-spin to a low-spin manganese configuration. In addition, the large ferromagnetic moment value immediately below the first-order transition at T_1 indicates that the ferromagnetic $B8_1$ structure also has a high-spin manganese moment. Therefore, the first-order transition involves a discontinuous change in the manganese spin state.

Secondly, the variation of the paramagnetic Curie temperatures of MnAs with pressure is positive in the orthorhombic phase and negative in the hexagonal phase. This difference in behavior has important implications vis-à-vis the applicability of the Bean-Rodbell model to the first-order transition in MnAs, as is discussed more fully in Sec. IV.

The experimental results discussed in parts A, B, and C of this section are summarized in the over-all magnetic-phase diagram of MnAs, which is given in Fig. 12.

IV. THERMODYNAMIC CONSIDERATIONS

As described in Sec. III we have measured the pressure dependence of the paramagnetic Curie temperature in both the hexagonal and orthorhombic phases, and have obtained $d\theta(B8)/dP=-12$°K/kbar and $d\theta(B31)/dP=+7$°K/kbar. According to the Bean-Rodbell (B-R) model

$$d\theta/dP=-T_0K\beta, \qquad (2)$$

where T_0 and β have been defined in Eq. (1) and $K=-V^{-1}(dV/dP)_T$ is the compressibility. According to DeBlois and Rodbell,[7] $T_0(B8_1)\cong 185$°K.[23] Although its value is unknown, the compressibility of MnAs is, of necessity, a positive quantity.[24] Therefore our experimental results lead directly to the conclusion that $\beta<0$ in the orthorhombic phase and $\beta>0$ in the hexagonal phase. This directly contradicts a fundamental assumption of the B-R model, namely, that β is constant through the transition. It therefore appears that this model, in its present simplified form, is not applicable to the MnAs transition.[25]

In order to account for the change in sign of $d\theta/dP$ through the transition, let us reconsider the initial

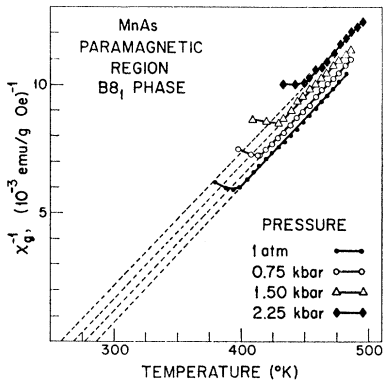

FIG. 10. Paramagnetic susceptibility curves of MnAs in the high-temperature hexagonal phase at the indicated pressures. Departure of curves from linearity demarcates transition temperature T_2.

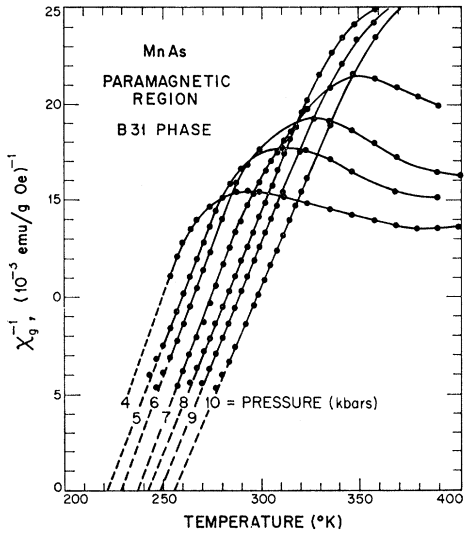

FIG. 11. Paramagnetic susceptibility curves of orthorhombic MnAs at the indicated pressures.

[23] Strictly speaking, this value refers to T_0*, as discussed in Ref. 7. To determine T_0, this value should be corrected for the effect of thermal expansion and the strain sensitivity of the magnetic-exchange interactions. In this case, the correction could lead to an increase of perhaps 20% in the value of T_0. This will not effect the discussion which follows.

[24] N. P. Grazhdankina, L. G. Gaidukov, K. P. Rodionov, M. I. Oleinik, and V. A. Shchipanov (Zh. Eksperim. i Teor. Fiz. **40**, 433 (1961) [English transl.: Soviet Phys.—JETP **13**, 297 (1961)]) have directly determined K in CrTe to be 2.2×10^{-3}/kbar. CrTe also has the NiAs structure. Values of K of the same order of magnitude have been inferred for MnAs in Refs. 5 and 7, but these results assume the B-R model to be valid through the transition.

[25] Inclusion of the volume dependence of the magnetic moment in the physical interpretation of β (Ref. 9) cannot alter this conclusion.

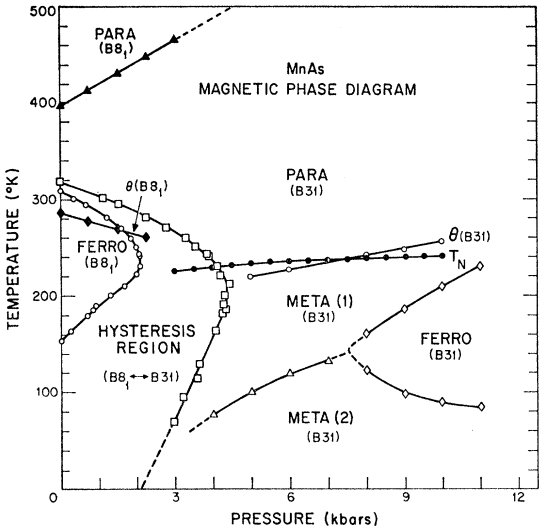

FIG. 12. Over-all magnetic-phase diagram of MnAs summarizing our experimental results.

assumptions of the B-R model, namely, that there is a single exchange interaction and that the elastic and magnetic properties are isotropic. The assumption of a single-exchange interaction constant is patently incorrect, being incompatible with the existence of a positive θ (or T_0) coupled with an antiferromagnetic Néel point T_N, as we have observed in the $B31$ phase of MnAs. Further, the fact that the volume change across the first-order transition all occurs in the hexagonal plane,[3] the distance between planes remaining essentially unchanged, indicates that the elastic properties exhibit hexagonal symmetry and are not isotropic. Hirahara *et al.*[26] have demonstrated highly anisotropic strain sensitivity of the magnetic-exchange interactions in MnP, which is isostructural with the $B31$ phase of MnAs. In MnP, changes in Curie temperature per unit stress along different crystallographic axes had unlike signs as well as absolute values that varied by over an order of magnitude. It therefore seems necessary to remove these assumptions present in the B-R model.

With an arbitrary number of exchange interactions J_{uv}, and different strain sensitivities $\beta_{uv}{}^i$ along $i=1$, 2, 3 coordinates, the free energy can be expressed in terms of arbitrary second-order elastic constants c_{ij}. The results are given in Appendix A. The variation of the Curie temperature as a function of pressure is obtained from the pressure derivative of Eq. (A9), which gives

$$\frac{d\theta}{dP}=-\frac{2S(S+1)}{3k}\sum_v z_{uv}J_{uv}{}^0\sum_{i=1}^{3}\sum_{j=1}^{3}\beta_{uv}{}^iK_{ij}, \qquad (3)$$

where the various terms have been defined in Appendix A. Since all the terms on the right-hand side of Eq. (3) are constants, it is clear that removal of the restrictions discussed above from the B-R model cannot lead to a change in sign of $d\theta/dP$ on going from the $B8_1$ to the $B31$ phase of MnAs.

Therefore, in order to account for the observed change in $d\theta/dP$ on the basis of Eq. (3), it would be necessary to impose the additional condition that the values of the K_{ij} terms be different in the $B8_1$ and $B31$ phases. Since the K_{ij} are functions of the elastic constants c_{ij}, and the interrelationships of the c_{ij} are different for the cases of hexagonal and orthorhombic symmetry (being more restrictive for hexagonal symmetry), it seems intuitively reasonable to have the set of K_{ij} change upon changing the crystal symmetry of a given material.

However, the existence of a second-order transition from hexagonal to orthorhombic symmetry at temperature T_2 implies that at this temperature there is a change in the strain symmetry with no concomitant discontinuity in the elastic constants. This requires extension of the free-energy calculations to include third-order elastic coefficients. As shown in Appendix B, it is then possible to encompass both hexagonal and orthorhombic strain symmetry within a single set of elastic coefficients. The pressure dependence of the Curie temperature, from the pressure derivative of Eq. (B6), is then

$$\frac{d\theta}{dP}=\frac{2S(S+1)}{3k}\sum_v z_{uv}J_{uv}{}^0\left[\beta_{uv}{}'{}^1\frac{d\eta_1}{dP}-\sum_{i=2}^{3}\beta_{uv}{}'{}^i\left(\frac{a_i}{\lambda_i}-\frac{\mathfrak{L}_{i11}}{\lambda_i}\eta_1\frac{d\eta_1}{dP}\right)\right], \qquad (4)$$

with the terms defined in Appendices A and B. Since the strain parameter η_1 is proportional to the orthorhombic distortion, $\eta_1=0$ corresponds to hexagonal symmetry. For that case, only the second term on the right-hand side of Eq. (4) is nonzero. This term, which is constant, corresponds to the right-hand side of Eq. (3).

With the introduction of an orthorhombic distortion, $\eta_1\neq 0$, and the solution for η_1 given by Eq. (B5) is valid. This leads to the appearance of two additional nonzero terms on the right-hand side of Eq. (4). The first of these introduces an abrupt and constant change in $d\theta/dP$. The last term, however, involves η_1, which is a function of both temperature and pressure. Therefore, it is theoretically possible to obtain a variation in the pressure dependence of the Curie temperature in the orthorhombic phase. However, within experimental accuracy, $d\theta(B31)/dP$ as taken from the values given in Table I appears to be constant over the range from 5 to 10 kbar. We therefore conclude that the nonlinearity introduced by the last term is too small to be observed experimentally.

The above considerations establish the necessary conditions for compatibility between the observed varia-

[26] E. Hirahara, T. Suzuki, and Y. Matsumura, J. Appl. Phys. 39, 713 (1968).

tion in $d\theta/dP$ and a model of strain-sensitive exchange effects giving rise to a first-order phase transition. They do not establish the sufficiency of these conditions as applied to MnAs. This will require knowledge of the elastic coefficients as well as detailed information regarding all the significant exchange interactions in this material. Furthermore, the difference between the manganese moment in the hexagonal and orthorhombic phases should also be taken into account. Although immaterial to the considerations above, this change in spin greatly complicates any quantitative analysis of the transitions between phases.

V. BAND-MODEL CONSIDERATIONS

It has been argued[9] that the sharp change in the manganese moment at T_1 is due to an equally sharp change in the intra-atomic exchange splitting, Δ_{ex}, of states of different spin, which is consistent with a critical Mn-Mn separation. To investigate this transition in detail, consider the schematic band structure for the d-state manifold shown in Fig. 13. It is assumed that the Fermi energy E_F lies in the gap between the top of the s-p bonding band and the bottom of s-p antibonding band, and there are four d electrons per manganese atom.

Localized d-electron orbitals in the $B8_1$ phase would have trigonal symmetry and would be associated with three distinct energy levels, labelled $a_1{}^T$, e^T, and e. The $a_1{}^T$ orbital is directed toward near-neighbor manganese atoms along the c axis; the two e^T orbitals toward near-neighbor cations in the basal plane; and the two e orbitals toward near-neighbor arsenic atoms. As discussed elsewhere,[8,9] the $a_1{}^T$ and e orbitals should be transformed into narrow-band collective-electron states, while the e^T orbitals should be transitional in character. For a sharply defined critical Mn-Mn separation of $a_0 \cong 3.7$ Å, the e^T orbitals would remain localized for larger Mn-Mn separations in the basal plane and become collective for smaller separations. At $T=T_2$, the lattice parameter is $a_0 \cong 3.7$ Å.[3]

One other concept is required. Narrow bands of a two-sublattice array (such as the linear chain along the c axis) tend to be split into bonding and antibonding states via the Coulomb energy U required to create polar states. This produces a deep minimum in the density of states where the band is half filled. In fact, spontaneous band antiferromagnetism splits a half-filled band in two. This means that with the Mn-Mn separation along the c axis shorter than in the basal planes, the bonding $a_1{}^T$ orbitals are all more stable than the corresponding e^T orbitals, and the antibonding $a_1{}^T$ orbitals overlap the e^T orbitals. In addition, if the $a_1{}^T$ orbitals are three-quarters filled and there is spontaneous-band ferromagnetism, then all the bonding $a_1{}^T$ states are filled and only the antibonding states of α spin are filled. In this situation there should again be a sharp minimum in the density-of-states-versus-energy curve for the $a_1{}^T$ band at the Fermi level E_F.

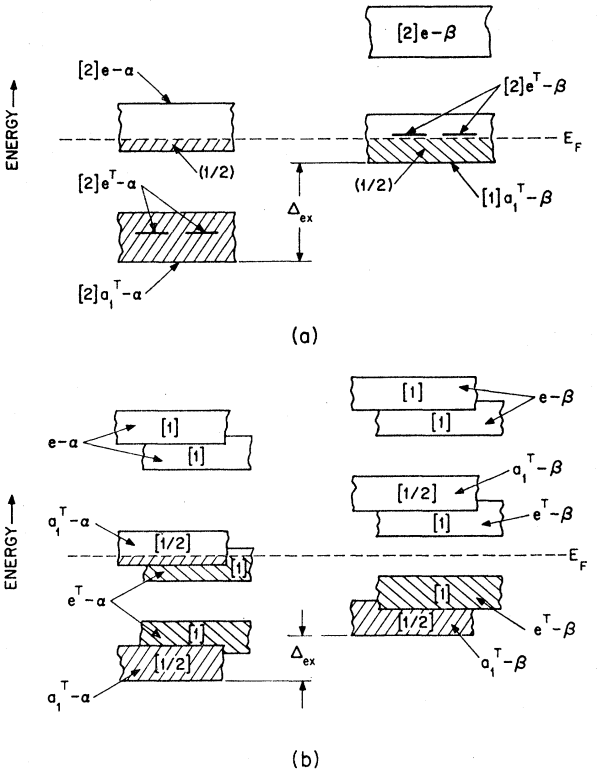

FIG. 13. Schematic one-electron band model for the d-state manifold of MnAs. The Fermi energy E_F is assumed to lie between filled and empty s, p bands which are not shown. The numbers in brackets and parentheses indicate the number of orbitals and electrons, respectively, per molecule in a given band. (a) Hexagonal ($B8_1$) phase; $\mu_{Mn}=3\mu_B$. (b) Orthorhombic ($B31$) phase; $1\mu_B<\mu_{Mn}<2\mu_B$, depending on magnitude of Δ_{ex}.

With these considerations, the properties of MnAs can be rationalized with the aid of Fig. 13(a). In the hexagonal $B8_1$ phase, where $a_0>3.7$ Å, the nearly localized e^T orbitals induce a large intra-atomic exchange splitting Δ_{ex} of states of different spin. To obtain approximate agreement with the observed saturation ferromagnetic moment value $\mu \cong 3.1\mu_B$ in the hexagonal $B8_1$ phase, it is assumed that the e^T orbitals of β spin, $e^T-\beta$, are empty and that the $a_1{}^T$ orbitals are three-quarters filled, giving a half-filled $a_1{}^T-\beta$ band. The relative stability of this configuration is assured if the $a_1{}^T-\beta$ band is actually split in two by the electrostatic energy U. With four outer d electrons, this requires that the Fermi energy E_F fall simultaneously in the $e-\alpha$ band and the $a_1{}^T-\beta$ band giving the configuration $(a_1{}^T-\alpha)^1(e^T-\alpha)^2(e-\alpha)^{1/2}(a_1{}^T-\beta)^{1/2}$, corresponding to $\mu=3\mu_B$. Further, with such a configuration, not only the Mn-Mn interactions along the c axis but also the Mn-As-Mn interactions should be ferromagnetic.[27] With half-filled e^T orbitals, on the other hand, the interactions within a basal plane would be antiferromagnetic, so that ferromagnetic order must induce an exchange-strictive expansion in the basal plane. The abrupt expansion observed in the basal plane at the

[27] J. B. Goodenough, J. Appl. Phys. 39, 403 (1968).

first-order transition is in agreement with this model, and definitively indicates that one of the strain-sensitive exchange parameters must involve the Mn-Mn interactions within this plane.

As the temperature is lowered through T_2, the e^T level broadens into a narrow band of collective-electron states, which tends to reduce the intra-atomic-exchange splitting Δ_{ex}. This results in a transfer of electrons from the $e-\alpha$ to the $e^T-\beta$ bands. In addition, the simultaneous distortion to the $B31$ symmetry further splits the ${a_1}^T-\alpha$ and ${a_1}^T-\beta$ bands, as well as splitting the $e^T-\alpha$ and $e^T-\beta$ bands in two. Thus the orthorhombic distortion causes the electron transfer to go from $e-\alpha$ to $e^T-\beta$ bands, and the occupancy of the ${a_1}^T-\beta$ band remains unchanged. (This is compatible with the observation that there is no discontinuity in the c axis at T_1.) As the temperature is lowered to $T=T_2-\Delta T$, electron transfer from the $e-\alpha$ bands goes to completion. This gives a spin-only moment of $2\mu_B$ provided Δ_{ex} is large enough to keep the Fermi energy E_F above the top of the ${a_1}^T-\alpha$ band. However, a further reduction in Δ_{ex} could completely fill the e^T bonding orbitals to give the band model shown schematically in Fig. 13(b), wherein the spontaneous atomic moment is $\mu\cong 1\mu_B$. In addition, the presence of $e^T-\beta$ electrons converts the Mn-Mn interactions within basal planes from antiferromagnetic to ferromagnetic or metamagnetic, since the number of electrons per e^T orbital is raised from one to between 5/4 and 3/2,[27] depending on the magnitude of Δ_{ex}. Therefore we can anticipate either ferromagnetism or metamagnetism in the $B31$ phase, the particular complex-spin configuration depending upon the relative filling of the ${a_1}^T$ and e^T bands. However, in the interval $T_2-\Delta T<T<T_2$, there may be a first-order transition back to the $B8_1$ phase with a discontinuous increase in a_0 to $a_0>3.7$ Å. In such a transition the e^T bands are reconverted to localized levels and the magnetic energy associated with a large Δ_{ex} is regained. Therefore the transition temperature must increase with applied external fields H_a, as has already been determined by DeBlois and Rodbell.[7]

Finally, the exchange-strictive expansion of the basal planes in the ferromagnetic $B8_1$ phase reduces the antiferromagnetic contribution to the total-exchange energy that determines the Curie temperature. Therefore the extrapolated Curie temperature T_c(ext) of the ferromagnetic $B8_1$ phase can be considerably larger than the paramagnetic Curie temperature $\theta(B8)$ determined from the paramagnetic susceptiblity. This may explain the experimental results in the $B8_1$ phases of MnAs, where it is found that the extrapolated ferromagnetic Curie temperature T_c(ext)$\cong$400°K, while the paramagnetic Curie point $\theta(B8)\cong$285°K.

ACKNOWLEDGMENT

We would like to thank Dr. W. H. Kleiner for helpful discussions regarding the transformation properties of elastic constants.

APPENDIX A

The stress-strain equilibrium conditions, to lowest order, are

$$S_i=\sum_j c_{ij}\epsilon_j, \tag{A1}$$

where $1\leq i, j\leq 6$. The c_{ij} are the elastic constants, and the ϵ_j represent linear strains along three mutually orthogonal axes for $1\leq j\leq 3$ and shear strains for $4\leq j\leq 6$. For the case wherein the applied stress is in the form of hydrostatic pressure P, the shear strains vanish identically at equilibrium, leaving

$$0=P+\sum_j c_{ij}\epsilon_j, \tag{A2}$$

where now the summation extends only over $1\leq j\leq 3$.

Bean and Rodbell[7] considered only an isotropic volume strain with a single-exchange interaction. Their expression for the Gibbs free energy per unit volume can be generalized to include multiple-exchange interactions and general strains as follows:

$$G_v=-m\mathbf{H}\cdot\sum_u \boldsymbol{\sigma}_u-\sum_{u,v}\bar{J}_{uv}{}^0(1+\sum_i \beta_{uv}{}^i\epsilon_i)\boldsymbol{\sigma}_u\cdot\boldsymbol{\sigma}_v$$
$$+\tfrac{1}{2}\sum_{i,j} c_{ij}\epsilon_i\epsilon_j+P\sum_i \epsilon_i-T\sum_{i,j}\alpha_j c_{ji}\epsilon_i-TS_{\text{spin}}, \tag{A3}$$

where $1\leq i, j\leq 3$. In the above equation,[28] the first term on the right-hand side represents the energy due to the interaction of the external field $\mathbf{H}$ with the sample, where m denotes the saturation moment of a single spin while $\boldsymbol{\sigma}_u$ is the thermodynamic expectation value of a unit vector describing the spin direction at site u. The second term corresponds to the exchange energy, where we have expressed the strain dependence of the exchange interaction between spins at the u and v sites, J_{uv}, by

$$J_{uv}=J_{uv}{}^0(1+\sum_i \beta_{uv}{}^i\epsilon_i), \tag{A4}$$

where $J_{uv}{}^0$ represents the uv exchange interaction in the unstrained sample ($T=P=0$), and the $\beta_{uv}{}^i$ directly relate the strain components ϵ_i to the change in the uv exchange interaction. Since $\boldsymbol{\sigma}_u$ and $\boldsymbol{\sigma}_v$ represent relative magnetizations, the spin magnitudes are included in $\bar{J}_{uv}=J_{uv}S_uS_v$, where the S_u are the spin quantum numbers. The third term of Eq. (A3) expresses the elastic energy of the lattice and the fourth is simply $P(V-V_0)/V_0$. The fifth term represents the lattice entropy, where we have followed the approximation of Bean and Rodbell.[7] The sixth term denotes the spin entropy.

[28] Although Eq. (A3) appears to represent a reasonable approximation of the Gibbs free energy per unit volume within either the $B8_1$ or $B31$ phase of MnAs, complications arise in applying it through the transition. As we have shown, the magnetic moment per manganese ion differs in the two phases. Therefore the values of m, $\bar{J}_{uv}{}^0$, and S_{spin} in the first, second, and sixth terms, respectively, should not be treated as constants through the transition. In order to simplify the problem, we have limited ourselves in the remainder of Appendix A to consideration of the transition from the ferromagnetic $B8_1$ phase to the paramagnetic state where, within the molecular-field approximation, $|\sigma|=0$.

Minimizing the free energy with respect to strain by taking the derivative of G_v with respect to ϵ_i and setting it equal to zero leads to the equilibrium condition

$$\sum_j c_{ij}\epsilon_j=\sum_{u,v}\bar{J}_{uv}{}^0\beta_{uv}{}^i\boldsymbol{\sigma}_u\cdot\boldsymbol{\sigma}_v-P+T\sum_j\alpha_j c_{ji}. \quad \text{(A5)}$$

The strain components which minimize the free energy are therefore

$$\epsilon_j=\sum_i K_{ji}\Big(\sum_{u,v}\bar{J}_{uv}{}^0\beta_{uv}{}^i\boldsymbol{\sigma}_u\cdot\boldsymbol{\sigma}_v-P+T\sum_k\alpha_k c_{ki}\Big), \quad \text{(A6)}$$

where K_{ji}=cofactor of c_{ij}/determinant c_{ij}.

Within the molecular field approximation, the Curie temperature θ is given by

$$\theta=(2/3k)S(S+1)\sum_v z_{uv}J_{uv}, \quad \text{(A7)}$$

where z_{uv} represents the number of v neighbors of a u atom, S is the spin quantum number, and k is Boltzmann's constant. From Eq. (A4),

$$\theta=(2/3k)S(S+1)\sum_v z_{uv}J_{uv}{}^0\Big(1+\sum_i\beta_{uv}{}^i\epsilon_i\Big) \quad \text{(A8)}$$

and, finally, substitution of Eq. (A6) with $|\sigma|=0$ at $T=\theta$ leads to the result

$$\theta=(2/3k)S(S+1)\sum_v z_{uv}J_{uv}{}^0\times\Big[1+\sum_i\beta_{uv}{}^i\sum_j K_{ij}\Big(-P+T\sum_k\alpha_k c_{ki}\Big)\Big]. \quad \text{(A9)}$$

APPENDIX B

The elastic energy of a material subjected to large strains can be expressed as

$$U-U_0=\tfrac{1}{2}\sum_{i,j}c_{ij}\epsilon_i\epsilon_j+\tfrac{1}{6}\sum_{i,j,k}L_{ijk}\epsilon_i\epsilon_j\epsilon_k, \quad \text{(B1)}$$

where i, j, and k all run from 1 to 6.[29] The matrices $\mathbf{c}$ and $\mathbf{L}$ are symmetric with respect to all permutations of their indices, and in addition must be invariant under the symmetry group of the crystal in its state U_0.

Let us choose the reference state U_0 for MnAs to be hexagonal and consider only terms with $1\leq i, j, k\leq 3$, since the shear strains must vanish. When ϵ_1 and ϵ_2 are defined as strains along the two orthorhombic axes lying in the hexagonal basal plane and ϵ_3 as the strain along the hexagonal axis, $c_{22}=c_{11}$ and $c_{23}=c_{13}$.[30] Diagonalization of this matrix yields eigenvalues λ_i associated with the eigenvectors $\hat{\eta}_1=2^{-1/2}(1,-1,0)$, $\hat{\eta}_2=(2+a^2)^{-1/2}(1,1,a)$, and $\hat{\eta}_3=(4+2a^2)^{-1/2}(-a,-a,2)$, where a and λ_i can be expressed in terms of the c_{ij}. We note in passing that the modes $\hat{\eta}_2$ and $\hat{\eta}_3$ retain hexagonal symmetry, while the mode $\hat{\eta}_1$ represents an orthorhombic distortion and is orthogonal (in lowest order) to the volume strain.

It is convenient to re-express the energy in terms of the amplitudes η_i of the strain modes $\hat{\eta}_i$, called the principal strains:

$$U-U_0=\tfrac{1}{2}\sum_i\lambda_i\eta_i{}^2+\tfrac{1}{6}\sum_{i,j,k}\mathfrak{L}_{ijk}\eta_i\eta_j\eta_k, \quad \text{(B2)}$$

where it can be shown, by virtue of the C_{6v} symmetry of the L_{ijk},[30] that $\mathfrak{L}_{122}=\mathfrak{L}_{133}=\mathfrak{L}_{123}=0$. If the above expression is substituted for the elastic energy in Eq. (A3) and the ϵ_i are written as linear combinations of the principal strains η_i, we obtain

$$G_v=\tfrac{1}{2}\sum_i\lambda_i\eta_i{}^2+\tfrac{1}{6}\sum_{i,j,k}\mathfrak{L}_{ijk}\eta_i\eta_j\eta_k+P\sum_i a_i\eta_i-T\sum_i\alpha_i'\lambda_i\eta_i-m\mathbf{H}\cdot\sum_u\boldsymbol{\sigma}_u-\sum_{u,v}\bar{J}_{uv}{}^0\times(1+\sum_i\beta_{uv}{}'{}^i\eta_i)\boldsymbol{\sigma}_u\cdot\boldsymbol{\sigma}_v-TS_{\text{spin}}, \quad \text{(B3)}$$

where it can be shown that $a_1'=0$ and also $\alpha_1'=0$, since $\alpha_2=\alpha_1$ for hexagonal symmetry.[30]

Ignoring the magnetic contributions to G_v for the present, as is valid in the paramagnetic state, we obtain the equilibrium conditions

$$\begin{aligned}0&=\eta_1(\lambda_1+\mathfrak{L}_{211}\eta_2+\mathfrak{L}_{311}\eta_3+\tfrac{1}{2}\mathfrak{L}_{111}\eta_1),\\ \eta_{i\neq1}&\cong T\alpha_i'-Pa_i/\lambda_i-\tfrac{1}{2}\mathfrak{L}_{i11}\eta_1{}^2/\lambda_i,\end{aligned} \quad \text{(B4)}$$

to lowest order in the $\eta_{i\neq1}$. Neglect of the $\mathfrak{L}_{ijk}$ would leave only the trivial solution $\eta_1=0$, for which the crystal must remain hexagonal. However, inclusion of the $\mathfrak{L}_{ijk}$ yields the alternative solution

$$\eta_1\cong-2[T(\mathfrak{L}_{211}\alpha_2'+\mathfrak{L}_{311}\alpha_3')-P(\mathfrak{L}_{211}a_2/\lambda_2+\mathfrak{L}_{311}a_3/\lambda_3)+\lambda_1]/\mathfrak{L}_{111} \quad \text{(B5)}$$

to lowest order. If $\lambda_1<0$ and $\mathfrak{L}_{111}>0$, then the orthorhombic state (with finite η_1) will be stable at zero temperature and pressure. However, Eq. (B5) shows that η_1 will then decrease with increasing temperature and will eventually become zero when $T=T_2$. The solution of Eq. (B5) for $\eta_1=0$ defines T_2 as a function of pressure. At all higher temperatures, where the value for η_1 given by solution of Eq. (B5) is negative, the hexagonal state ($\eta_1=0$ solution) will remain stable unless sufficient pressure is applied.

Finally, the procedures which led to Eq. (A9) now yield

$$\theta=\frac{2}{3k}S(S+1)\sum_v z_{uv}J_{uv}{}^0\Big[1+\beta_{uv}{}'{}^1\eta_1+\sum_{i=2}^{3}\beta_{uv}{}'{}^i\Big(T\alpha_i'-P\frac{a_i}{\lambda_i}-\tfrac{1}{2}\eta_1{}^2\frac{\mathfrak{L}_{i11}}{\lambda_i}\Big)\Big], \quad \text{(B6)}$$

where it is to be remembered that η_1 is identically zero for $T>T_2$, but is given by Eq. (B5) for $T<T_2$. Consequently $d\eta_1/dP$ will be discontinuous at $T=T_2$. In turn, this could produce a discontinuity in $d\theta/dP$, as evaluated from Eq. (B6), and could change its sign.

[29] See, for example, S. Bhagavantum, *Crystal Symmetry and Physical Properties* (Academic Press Inc., New York, 1966), pp. 126–156.

[30] F. G. Fumi, Phys. Rev. **86**, 561 (1952).